Chapter

Ultra-Low Temperature Chillers for Semiconductor Manufacturing Process

Jung-In Yoon, Chang-Hyo Son, Sung-Hoon Seol and Ji-Hoon Yoon

Abstract

The growth of the semiconductor market and advancement of manufacturing technology have led to an increase in wafer size and highly integrated semiconductor devices. The temperature of the supplied cooling medium from the chiller that removes the heat produced in the semiconductor manufacturing process is required to be at a lower level because of the high integration. The Joule-Thomson cooling cycle, which uses a mixed refrigerant (MR) to produce the cooling medium at a level of −100°C required for the semiconductor process, has recently gained attention. When a MR is used, the chiller's performance is heavily influenced by the composition and proportions of the refrigerant charged to the chiller system. Therefore, this paper introduces a cooling cycle that uses an MR to achieve the required low temperature of −100°C in the semiconductor manufacturing process and provides the results of simple experiments to determine the effects of different MR compositions.

Keywords: Semiconductor etching process, Mixed refrigerant refrigerator, Refrigerant mixing ratio, Ultra low temperature, Joule-Thomson cycle

1. Introduction

Because of the growth of the semiconductor market and the global competition among many companies of the United States, Taiwan, South Korea, etc., investment and interest in related industries are increasing [1]. As a result of this trend, there is an increased demand for chillers, which are temperature control systems used in the semiconductor manufacturing process, and the research into chillers is also progressing actively [2].

As shown in **Figure 1** [3], semiconductor manufacturing process consists of eight major processes, including wafer manufacturing, oxidation, photolithography, etching, and deposition [4]. Etching, one of the eight major semiconductor processes, is a process that removes unnecessary parts in the sketch of circuit drawn in the photolithography process [5]. A semiconductor etcher is a device used to etch circuit patterns formed on wafers. The typical method is to create plasma gas with excellent etching properties and etch a specified part of the wafer [6, 7]. Here, there might be a risk of an excessive rise in wafer temperature when it is exposed to the high temperature of the plasma [8]. Therefore, general etching devices cool

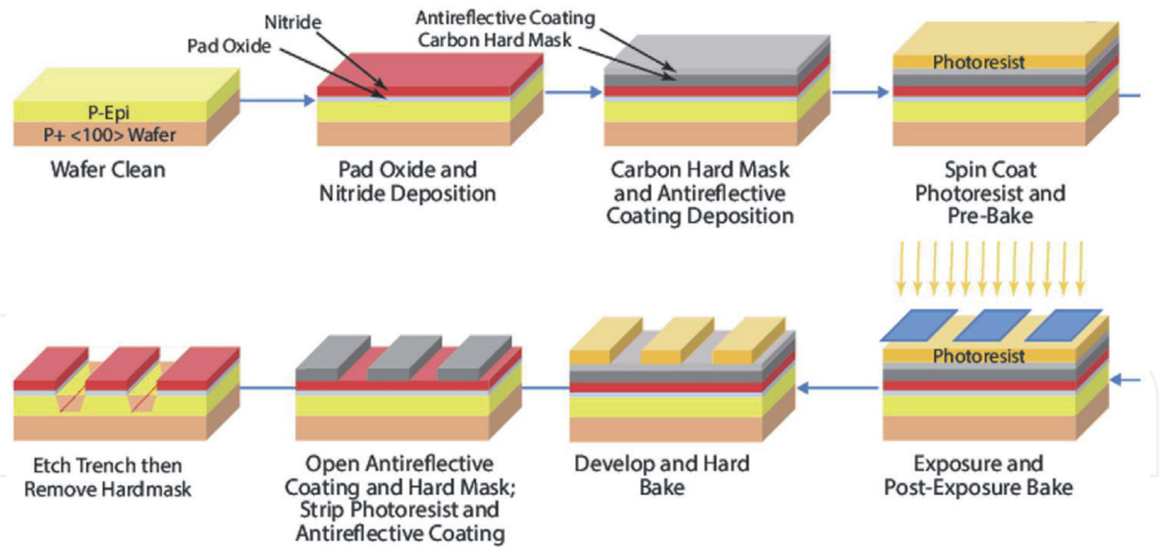

Figure 1.
Manufacturing process of semiconductors [3].

the wafers by circulating the cooling medium inside the electrostatic chuck (ESC) where the wafers are installed [9].

On the contrary, because of the high integration of semiconductor circuit patterns, the line width of circuits is becoming smaller [10]. The temperature of ESC in the 20 ~ 30 nm line-width etching process is room temperature, but the −20°C temperature level is primarily used at the 10 nm level. The etching processes that require a lower temperature are trending especially at the fine level of 5 ~ 7 nm process. Therefore, there is a growing demand for the ultra-low temperature etching process, which involves performing etching while maintaining the temperature of substrates below −100°C. If etching is performed in the ultra-low temperature domain, the spontaneous reaction is suppressed, enabling anisotropic etching. However, this kind of process has disadvantages in that implementation is difficult in terms of the equipment and environment for maintaining the ultra-low temperature of substrates, and the energy consumption is high.

To achieve the low temperature of −100°C, various cycles such as, two-stage cascade cycle, Joule-Thomson cycle, and auto-cascade cycle are used. Joule-Thomson coolers are used in many fields because they have a simpler structure and are easier to manufacture and operate compared with the two-stage cascade cycle. However, the main disadvantage of Joule-Thomson coolers is their low efficiency, which is caused by irreversibility because of the high-pressure rate and wide temperature range. This problem can be resolved by using a mixed refrigerant (MR). **Figure 2** shows the refrigeration effect of a single cooling medium according to the working pressure. Nitrogen or argon, which is a low boiling point cooling medium, requires a higher pressure to obtain the cooling calories compared to propane or ethane, which is a high boiling point cooling medium. In the case of nitrogen, for example, a working pressure of approximately 24.6 MPa is required to obtain a cooling calorie of 1,000 J/mol, whereas, in the case of propane, the working pressure may be at a level of approximately 0.79 MPa, showing a large difference [11]. In fact, if an MR is created by combining nitrogen, argon, methane, krypton, ethane, propane, etc., the cooling calorie of 1,000 J/mol can be obtained below the working pressure of 2.5 MPa.

Therefore, this paper introduces a Joule-Thomson cooler that uses an MR to achieve the low temperature of −100°C required in the semiconductor manufacturing process.

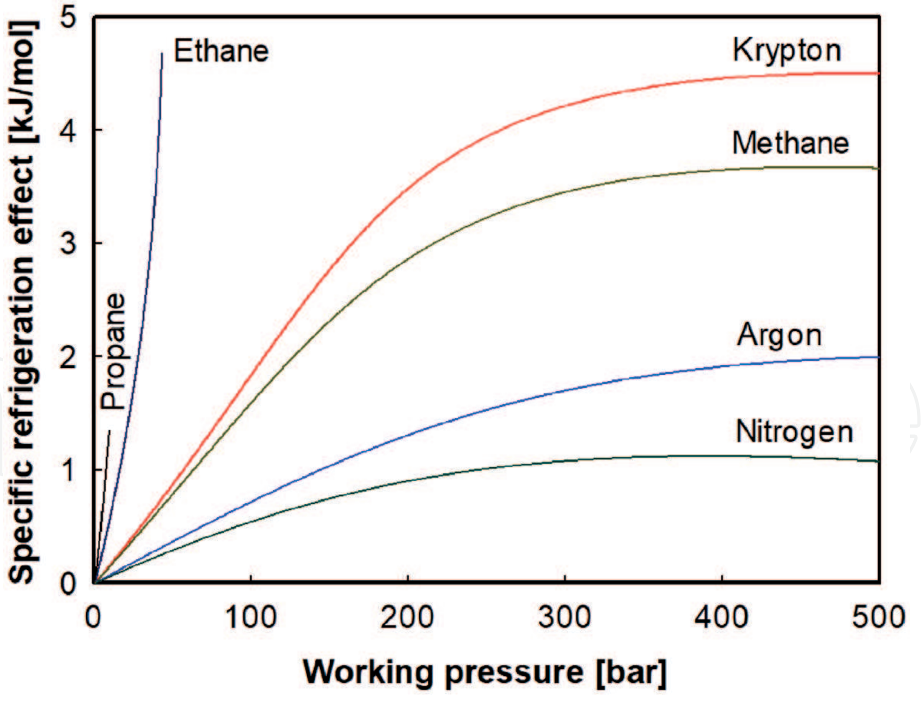

Figure 2.
Variation of specific refrigeration effect according to operation pressure [11].

2. Refrigeration cycles for ultra-low temperature

As aforementioned, a two-staged cascade cycle, Joule-Thomson cycle, etc. are used to achieve the low temperature of −100°C. This section introduces several refrigeration systems that are commonly used to achieve an ultra-low temperature [12].

2.1 Single mixed refrigerant (MR) refrigerator

A single MR refrigerator is a refrigerator that can achieve temperatures of −100°C or lower and has the advantage of having fewer mechanical elements, and it can be miniaturized. Because of these advantages, single MR refrigerators have been widely used in the semiconductor industry, which requires low-temperature refrigerators that can be operated reliably for an extended period. A single MR refrigerator has a single-stage refrigeration cycle that includes an intermediate heat exchanger, and it is configured as shown in **Figure 3**.

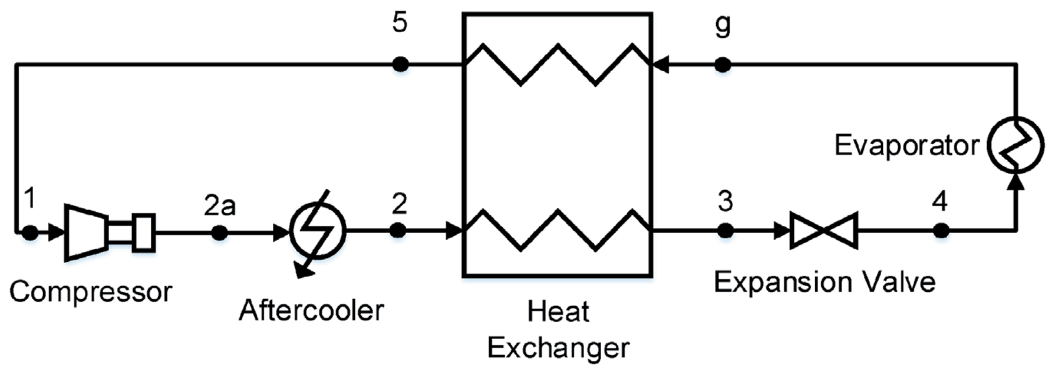

Figure 3.
Schematic diagram of joule-Thomson refrigeration (single MR) cycle.

The specific working principle of single MR refrigerators is as follows. The refrigerant vapor sucked by the compressor flows into the aftercooler in a state of high temperature and high pressure through the compression process (1–2a). The refrigerant vapor is then cooled to ambient temperature through heat exchange with the heat exchanging medium at room temperature (2a–2), and flows into the intermediate heat exchanger. Here, the refrigerant, which is in a vapor state at high pressure (2–3), is condensed through the heat exchange with a two-phase refrigerant (g–5) of low temperature and low pressure, and is transformed into a refrigerant of high pressure and low temperature. The high-pressure, low-temperature refrigerant that has passed through the intermediate exchanger passes through the expansion valve and transforms into a two-phase refrigerant of low temperature and low pressure because the pressure and temperature are decreased by the Joule-Thomson effect (3–4). Following this, the low-temperature, low-pressure refrigerant absorbs heat from the evaporator (4–g), passes through the intermediate heat exchanger, and is sucked into the compressor to complete the cycle.

The selected refrigerant type and composition proportions of the MR used in the single MR refrigerator vary depending on the evaporation temperature and operating conditions of the system. The evaporation temperature of the MR decreases as the proportion of low boiling point refrigerant increases, and the refrigeration capacity increases as the proportion of high boiling point refrigerant increases. Furthermore, as the two-phase sections of the selected refrigerants overlap, the time for reaching the target evaporation temperature decreases. The target evaporation temperature may not be reached if the selected composition proportions used in the MR are not appropriate, resulting in a stagnant temperature. Therefore, a specific method is required to select appropriate composition proportions of the MR. To select the composition proportions of an actual MR, it is essential to conduct experiments to validate various composition proportions selected theoretically.

2.2 Cascade mixed refrigerant (MR) refrigerator

A cascade MR refrigerator is a system that applies the Joule-Thomson cycle, in which the MR is applied to the two-stage cascade refrigeration system. With the active progress of the semiconductor market, the demand for refrigerators has increased, and related studies are an increasing trend. As mentioned, the cascade MR refrigerator includes an intermediate heat exchanger in the low-stage cycle of a two-stage refrigeration system. **Figure 4** shows the schematic diagram of the device.

The cascade MR refrigerator cycle is divided into high-stage and low-stage cycles, similar to a typical two-stage refrigeration cycle. First, the flow of the refrigerant in the high-stage cycle is introduced. The high-temperature, high-pressure vapor refrigerant discharged from the high-stage compressor becomes saturated or sub-cooled liquid as it passes through the condenser (1–2). The liquid refrigerant that passed through the expansion valve (2–3), then transforms into a two-phase low-temperature and low-pressure refrigerant. It flows into the cascade heat exchanger and exchanges heat with the refrigerant flow of the low-stage cycle (3–4). In other words, from the perspective of the low-stage cycle, the cascade heat exchanger serves as the aftercooler of the previously introduced single MR. Next, the flow of the refrigerant in the low-stage cycle is discussed. The refrigerant discharged from the low-stage compressor in a state of high-temperature, high-pressure vapor is partially condensed (5–6), which is then condensed into a fully liquid refrigerant through the internal heat exchange in the intermediate heat exchanger (6–7) and passes through the expansion valve (7–8). The liquid refrigerant that has passed through is in a state of low temperature and exchanges heat with the brine

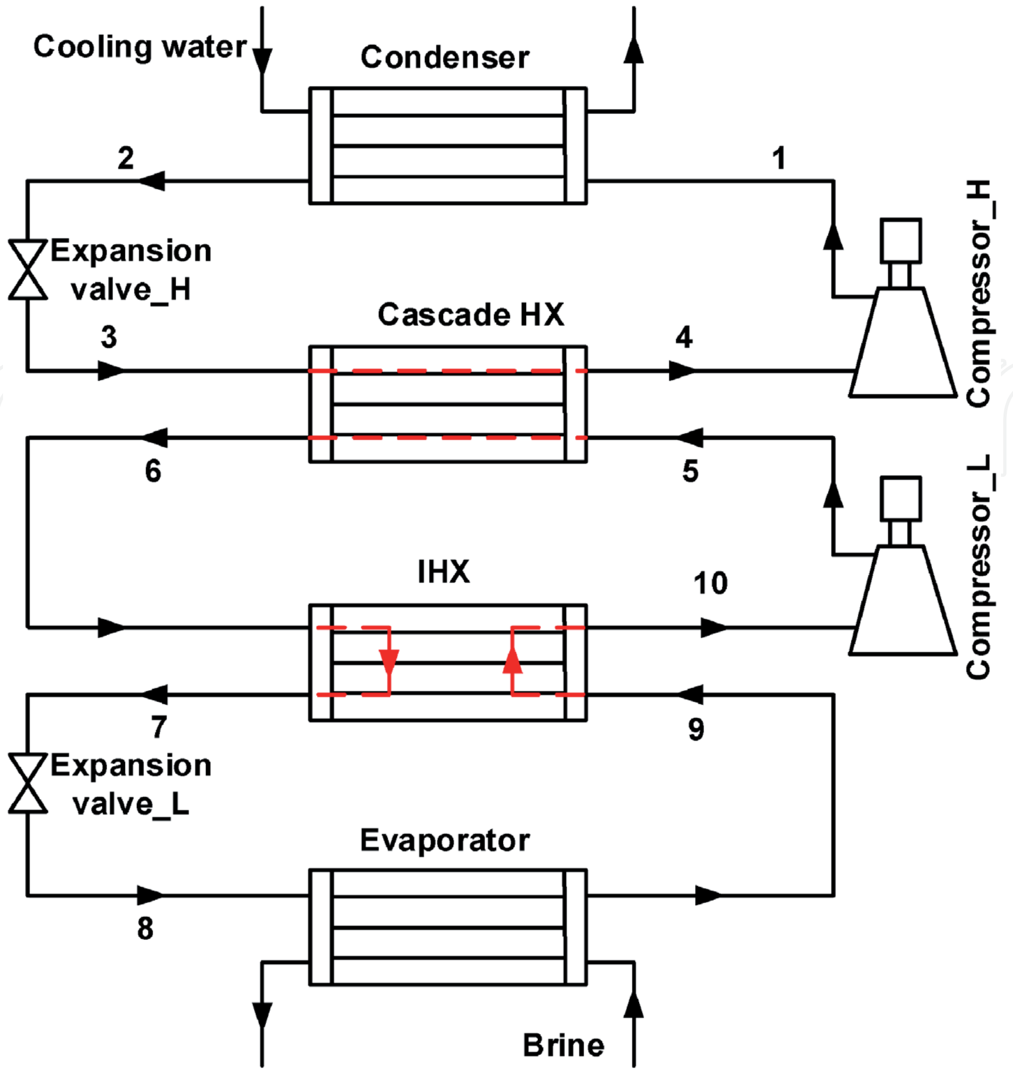

Figure 4.
Schematic diagram of cascade MR refrigeration cycle.

in the evaporator, resulting in partial evaporation (8–9). Complete evaporation occurs as the intermediate heat exchanger absorbs the heat from the high-pressure refrigerant (9–10). The evaporated refrigerant is sucked by the compressor, causing the cycle to repeat itself (10–5).

Meanwhile, it is required to explain the concept of Joule-Thomson cooling capacity, which is an important concept in studying the refrigerant composition in the MR refrigeration cycle. **Figure 5** shows an example of the refrigeration cycle using a single refrigerant for clarity. The enthalpy difference occurring when expanding from a high pressure to a low pressure along the isotherm is referred to Joule-Thomson cooling capacity. **Figures 6** and **7** show the Joule-Thomson cooling capacity of various refrigerants used in the composition of MR at each temperature point. For the refrigerants used in the analysis, **Table 1** shows the normal boiling point, global warming potential (GWP), ozone depletion potential (ODP), and the refrigerant safety group through the American Society of Heating, Refrigerating and Air-Conditioning Engineers (ASHRAE) 2009 [14].

As shown in **Figure 6** [13], in general, a refrigerant with a low standard boiling point has a small enthalpy difference, and a refrigerant with a high standard boiling point has a large enthalpy difference. If the temperature to be reached is low, then a refrigerant with a low standard boiling point should be used. However, because the temperature must be reduced from room temperature to a low-temperature region, a refrigerant with a high boiling point should be mixed to utilize advantage

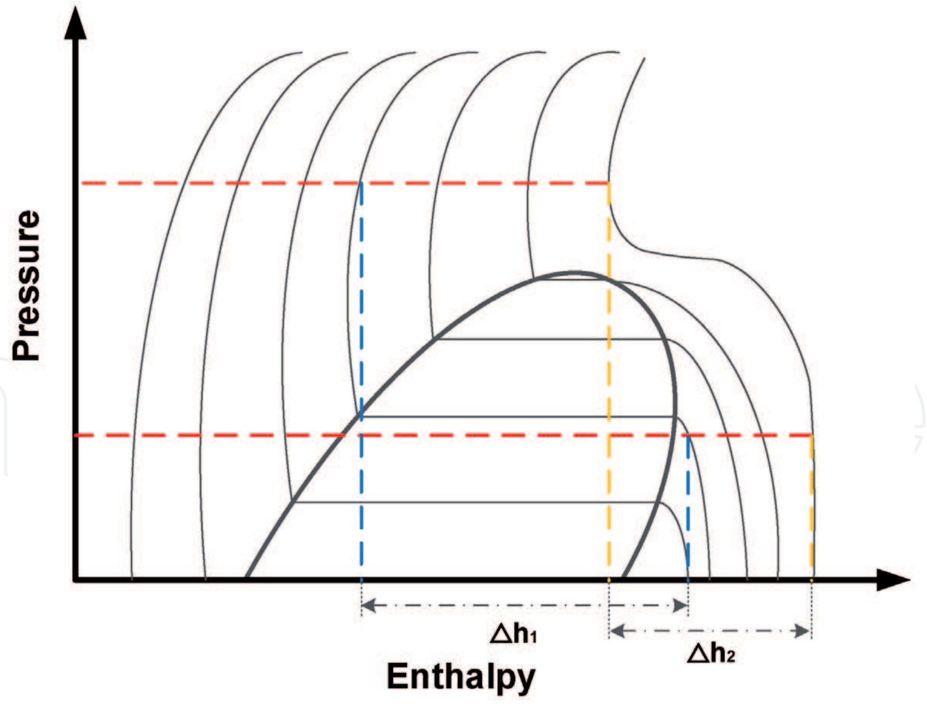

Figure 5.
P-h diagram of pure refrigerant for explaining joule-Thomson effect.

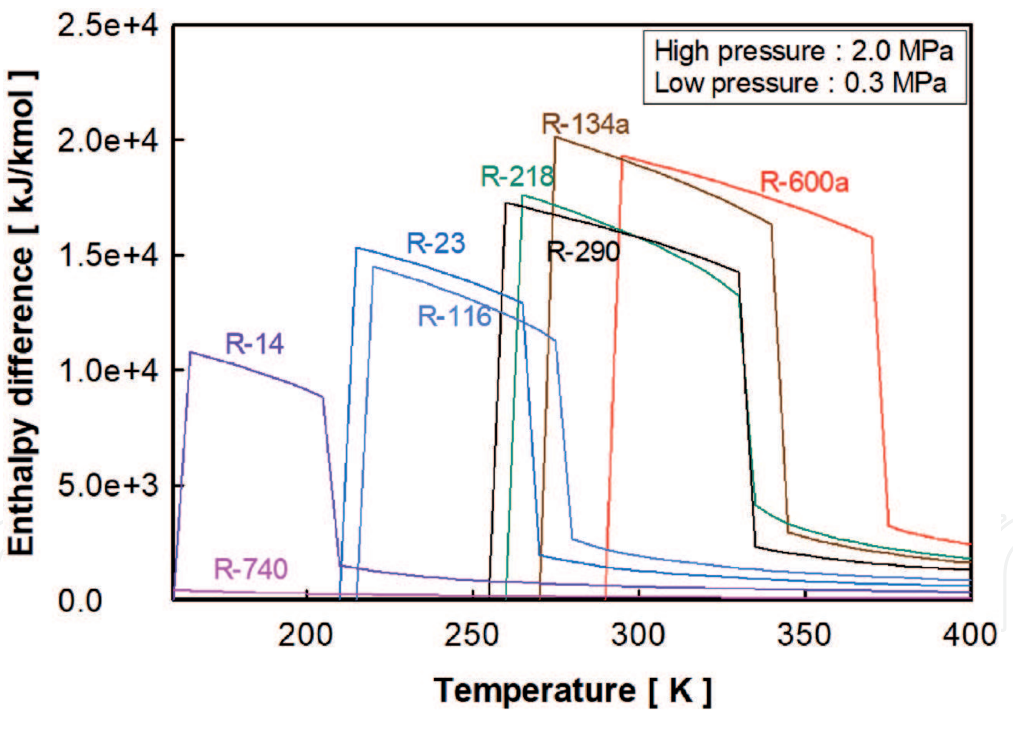

Figure 6.
Enthalpy difference according to temperature in kJ/kmol unit [13].

of a large enthalpy difference of it. In other words, a refrigerant with a low boiling point and that with a high boiling point should be mixed appropriately to satisfy the target cooling capacity and temperature simultaneously.

Figure 7 shows the enthalpy difference per unit mass for the same refrigerants by converting the y-axis from the unit mole to the unit mass. The refrigerants with high enthalpy differences, such as i-Butane (R600a) and propane (R290) refrigerants, which are hydrocarbon (HC) refrigerants, appear prominently regardless of the standard boiling point. These HC refrigerants have a characteristic that the molecular weight is small compared with other refrigerants, and when it is

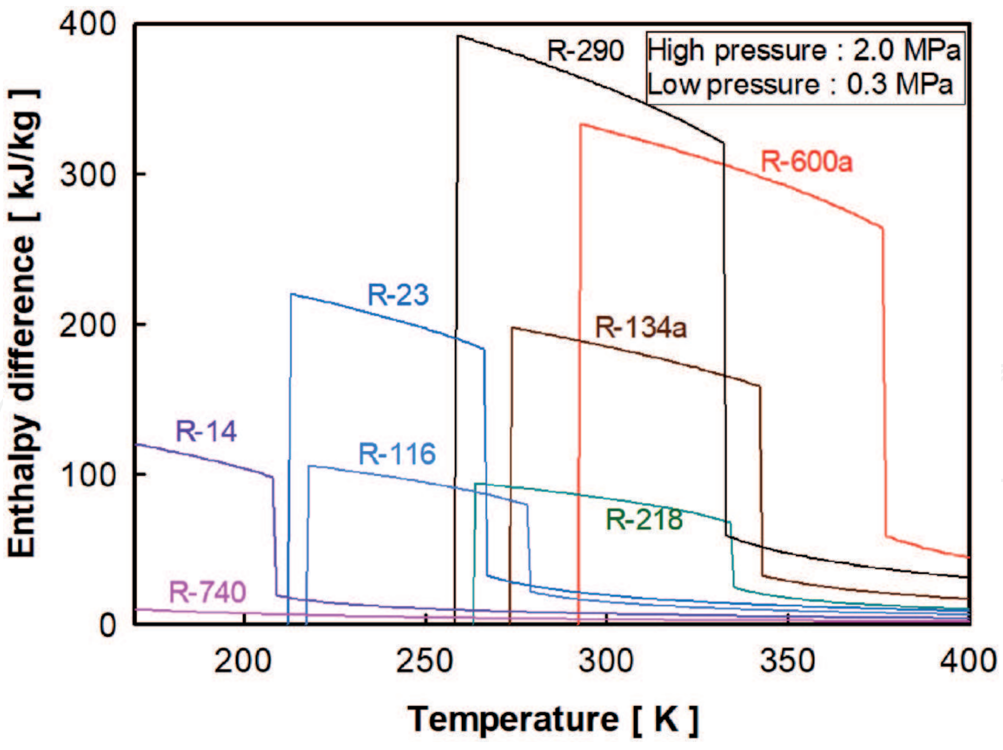

Figure 7.
Enthalpy difference according to temperature in kJ/kg unit [13].

Type	Refrigerant	Normal boiling point	GWP	ODP	Safety group	Molecular weight
HC	R-600a	−11.7	3	0	A3	58.122
HFC	R-134a	−26.3	1,430	0	A1	102.03
PFC	R-218	−36.7	8,830	0	A1	188.02
HC	R-290	−42.1	3.3	0	A3	44.096
PFC	R-116	−78.2	12,200	0	A1	138.01
HFC	R-23	−82.1	14,800	0	A1	70.014
PFC	R-14	−127.8	7,390	0	A1	88.010

Table 1.
Properties information of various refrigerants [14].

represented by the unit mass, a larger number of moles is included. Therefore, HC refrigerants can have larger enthalpy differences.

3. Experimental system and methodology

This section describes the experimental system and method of the cascade MR refrigerator, which is one of several refrigeration systems commonly used to achieve the ultra-low temperature introduced in Section 2.

Figure 8 shows the schematics of the experimental system, which is divided into low and high stage cycles. The high-stage cycle comprises of a compressor, condenser, expansion valve, and cascade heat exchanger, while the low-stage cycle comprises of a compressor, expansion tank, pre-cooling heat exchanger, cascade heat exchanger, intermediate heat exchanger, expansion valve, and evaporator. The cooling water side consists of an isothermal bath, process chilled water (PCW) pump, and inverter, and the flow rate of the cooling water is adjusted by controlling

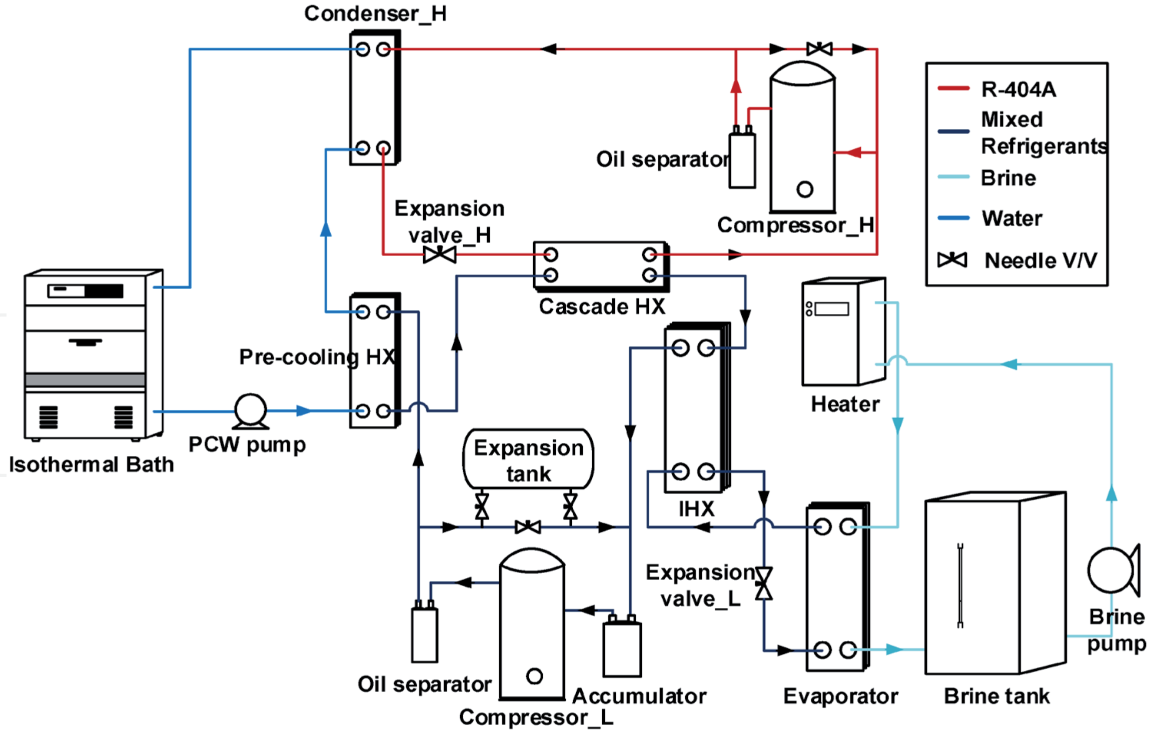

Figure 8.
Schematics of experimental system of cascade MR refrigerator.

the number of revolutions. The brine side consists of a brine tank, brine pump, inverter, and heater. The inverter also controls the flow rate of the brine, and the load is controlled using the heater in the brine tank.

Figure 9 explains the use of the pre-cooling heat exchanger, which was not mentioned in the aforementioned basic description of the cycle. The pre-cooling heat exchanger uses the cooling water going into the condenser of the high-stage cycle to primarily cool the high-temperature, high-pressure refrigerant discharged from the compressor of the low-stage cycle, and it handles a portion of the aftercooler capacity. A simulation analysis was performed to determine whether to use the pre-cooling heat exchanger. It should be noted that its use is accountable for a portion of the capacity handled by the aftercooler, and simultaneously has an adverse effect on the temperature of the cooling water entering the condenser of the high-stage cycle. The results of the simulation analysis show that the application of the pre-cooling heat exchanger increases the coefficient of performance (COP) by approximately 10% from 0.289 to 0.316. The actual device produced and experimented based on this is shown in **Figure 10**.

The experiments were carried out under the conditions shown in **Table 2** to determine the performance characteristics according to the MR composition of the cascade MR Joule-Thomson refrigerator that uses the MR as the working fluid. Cooling water of 18°C flows through the pre-cooling heat exchanger at 22 L/min and is supplied to the high-stage condenser, and the brine entering the evaporator is supplied at a constant flow rate of 40 L/min. The compressor selected was a standard commercial compressor. The discharge pressure should not exceed 3 MPa, and the suction pressure should be maintained above 0.1 MPa, according to the operational constraints of the compressor. For reference, if the suction pressure is in a vacuum state, the oil supply in the compressor may not be smooth and moisture may enter. Therefore, the suction pressure of the compressor must be higher than vacuum pressure. To prevent the carbonization of the compressor oil, the discharge temperature is limited to be within 120°C.

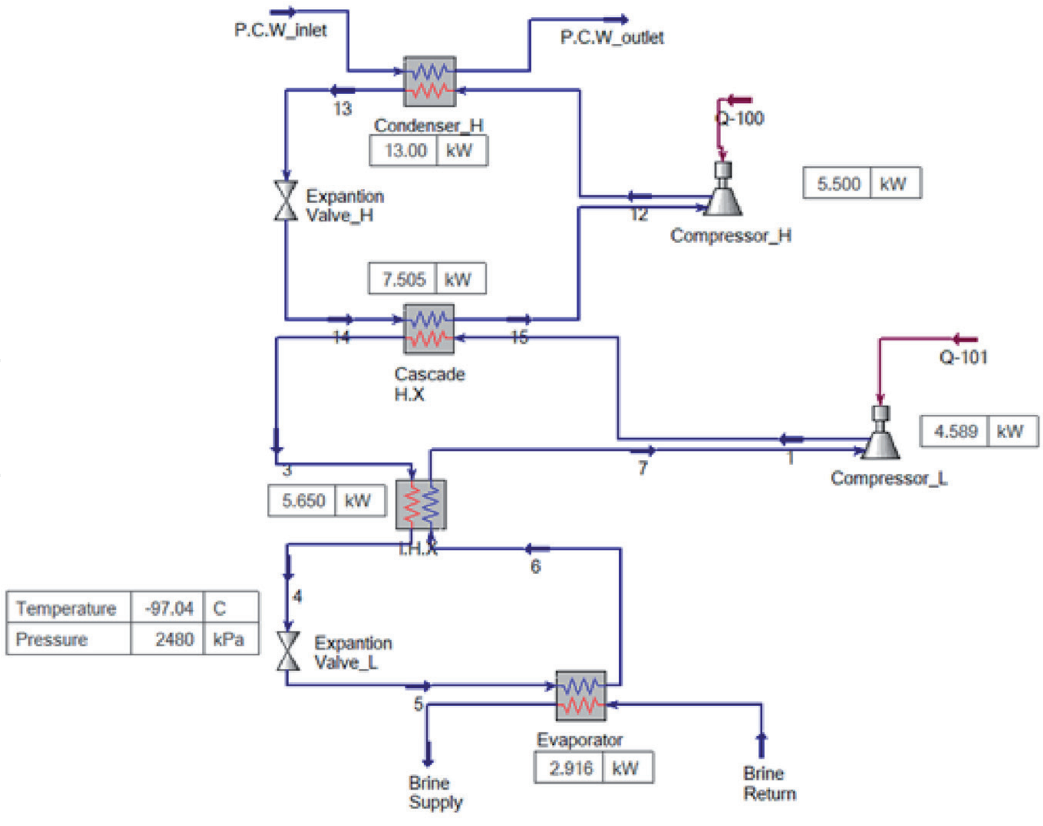

(a) without pre-cooling heat exchanger

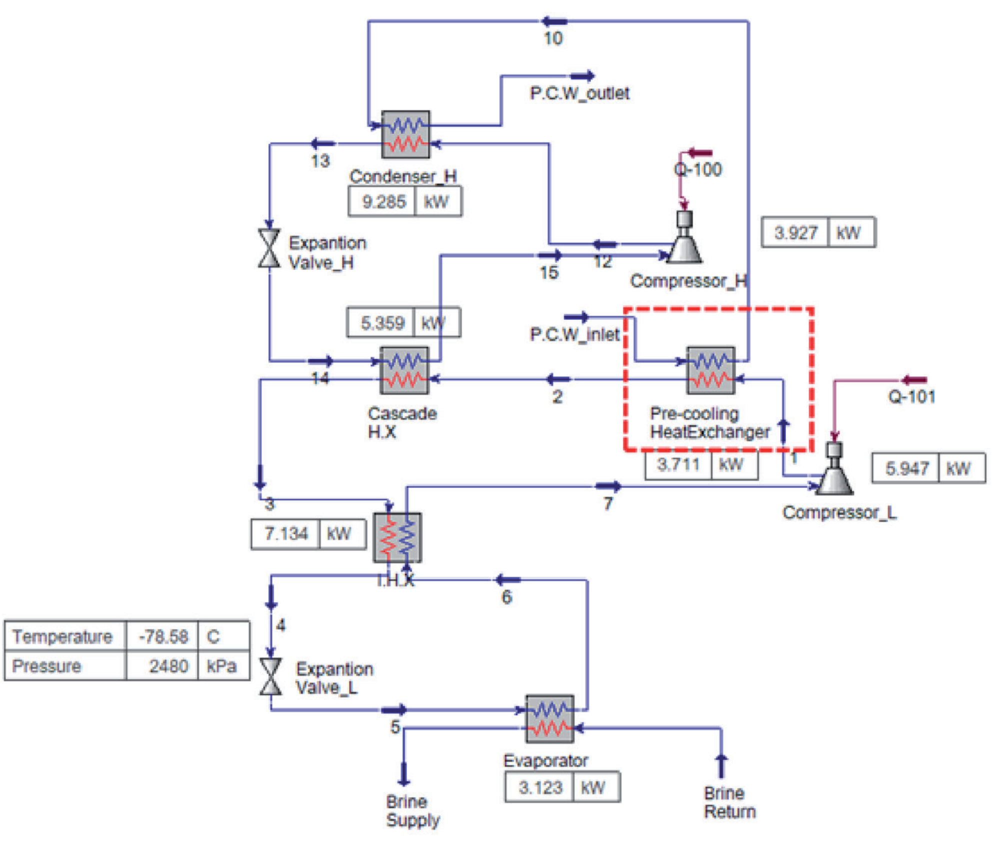

(b) with pre-cooling heat exchanger

Figure 9.
Comparison of cascade MR refrigerator with and without pre-cooling heat exchanger.

Figure 10.
Experimental device of cascade MR refrigerator.

Parameter	Value	Unit
Cooling water inlet temperature	18	°C
Cooling water volume flow	22	L/min
Brine volume flow	40	L/min
Brine supply temperature	−100	°C
Compressors discharge pressure constraint	3.0	MPa
Compressors discharge temperature constraint	120	°C
Compressor_L suction pressure constraint	0.1	MPa

Table 2.
Summary of experimental conditions.

The following method was used under the aforementioned experimental conditions. If the high-stage cycle reaches the target temperature, the compressor of the low-stage cycle is started. To prevent excessive pressure buildup, the valves installed before and after the expansion tank are opened during the process. The brine pump is

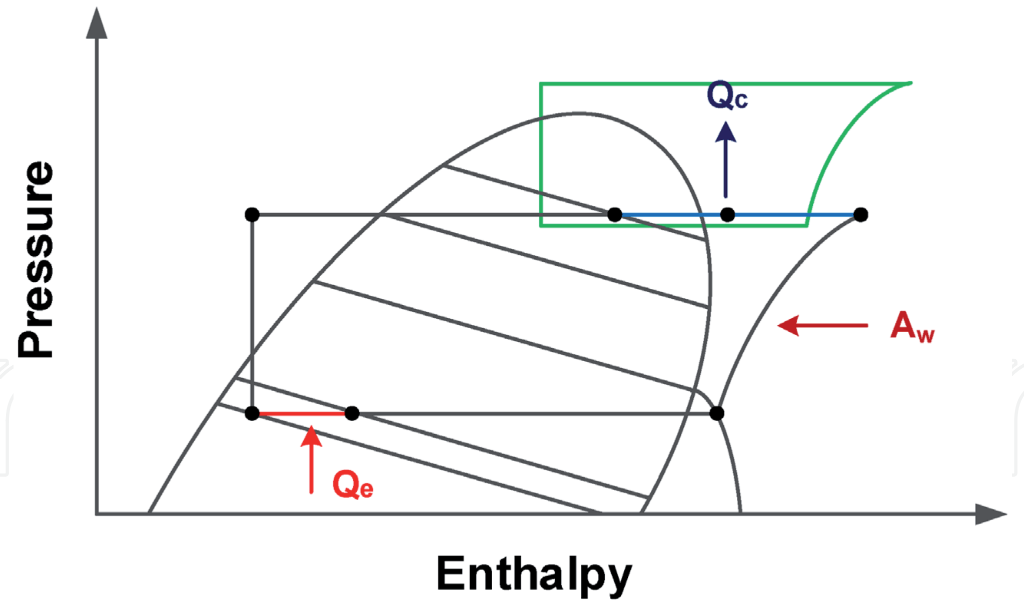

Figure 11.
P-h diagram of cascade MR refrigerator.

operated as soon as the compressor starts, thereby exchanging the heat at the evaporator. Following this, the opening of the expansion valve is controlled in such a way that the suction pressure of the compressor does not drop to or below the atmospheric pressure, until the target temperature is reached. As the target temperature is approached, the temperature of the low-pressure side stream entering the intermediate heat exchanger decreases, and accordingly, the pressure of the high-pressure side stream decreases. To solve this problem, the valve of the pipe connected to the compressor suction tube and the expansion tank is opened to inject the refrigerant to maintain the pressure. If the target temperature is reached, the load of the heater in the brine tank is gradually increased, and if the steady state is reached, the cooling capacity, including the load put on the heater and the heat generation pump, is measured.

Figure 11 shows the P-h diagram of the cascade MR refrigerator. The working fluid of the low-stage cycle consists of MR. When the flow rate of the cooling water entering the pre-cooling heat exchanger is sufficient, primary cooling proceeds up to the temperature of the cooling water, and the outlet temperature of the cascade heat exchanger is determined based on the evaporation temperature of the high-stage cycle. Here, when the low-stage cycle is viewed as a system, the sum of the cooling capacity at the evaporator and the work put into the compressor should be the same as the sum of the heat exhausted by the pre-cooling heat exchanger and the cascade heat exchanger. As the capacity of the pre-cooling heat exchanger and the aftercooler increases, the capacity of the evaporator increases. Because of its characteristics, the Joule-Thomson cycle using MR has a temperature gradient within the two-phase region, and the refrigerant temperature at the aftercooler outlet is limited to the temperature level of the cooling water. Therefore, in this study, the evaporator of the high-stage cycle, that is, the cascade heat exchanger, is used as the aftercooler of the low-stage cycle to increase the cooling capacity of the evaporator.

4. Experimental results and discussions

This section provides a brief overview of the data obtained using the experimental device of the cascade MR refrigerator introduced in Section 3. The specific composition proportions of the MRs below are not specified because they are protected by patent rights. In terms of changing the composition proportions, the total charging mass of MR was kept constant, and the mass proportions of the high boiling point refrigerants.

R290 and R600a were adjusted. In other words, the mass of three different types of refrigerants was increased by the same proportion as the reduced charging amount of the high boiling point refrigerant, and the total charging amount of the MR remained constant [15].

4.1 Experiments with MR compositions of R290, R116, R23, and R14

Figure 12 shows the compressor discharge temperature and suction temperature, evaporator inlet temperature, and expansion valve inlet temperature according to the operating time in the refrigerant's initial composition proportion (R290, R116, R23, and R14) state. The device was operated by applying the MR composed of the above four refrigerants, and the opening of the expansion valve was controlled according to the rapid pressure change. Here, the temperature was decreased while leaving the suction valve of the expansion tank open, and as the target temperature was reached, the valve was closed, and the brine heater was operated.

The experiment was conducted while adjusting R290 in a mass fraction range of 5–50%, as shown by MR1–MR8, to examine the performance of the device based on the proportion change of the high boiling point refrigerant (R290) in the refrigerant charging amount of the same mass. The charging amount of R290 was the highest in MR1 and the lowest in MR8. **Figure 13** shows the compressor discharge and suction temperature, evaporator inlet temperature, and expansion valve inlet temperature based on the composition ratio of R290. When the mass ratio of R290 decreased, the compressor suction temperature increased from −67.8°C to −48.2°C. In both cases of MR7 and MR8, the expansion valve inlet temperature was clearly high when the mass fraction of the high boiling point refrigerant dropped below a certain level. However, the evaporator inlet temperature after going through the expansion valve was between −109.2 and − 106.7°C, showing no significant effect.

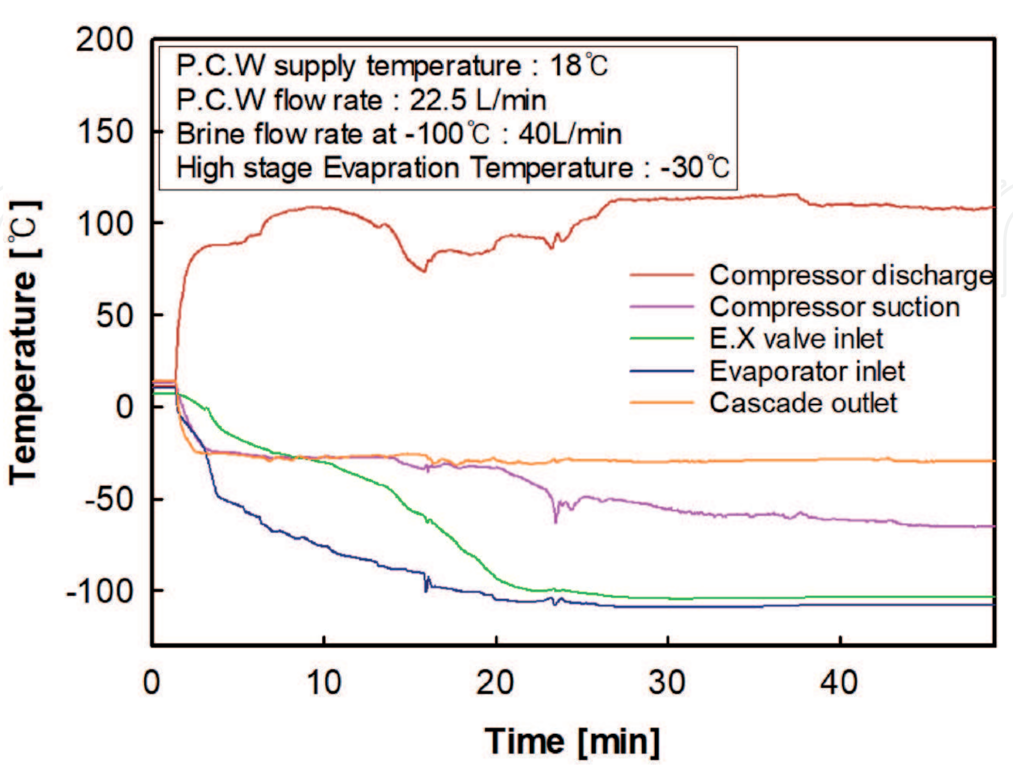

Figure 12.
Transient temperature of each measuring point (including R290).

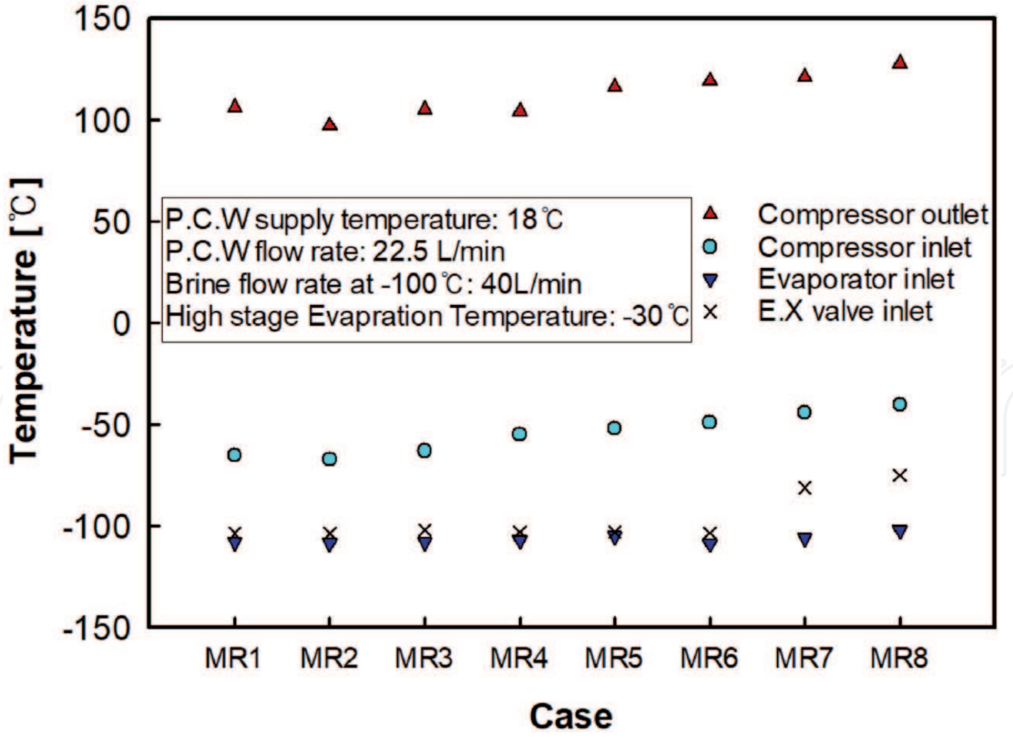

Figure 13.
Temperature comparison of various refrigerant composition cases (including R290).

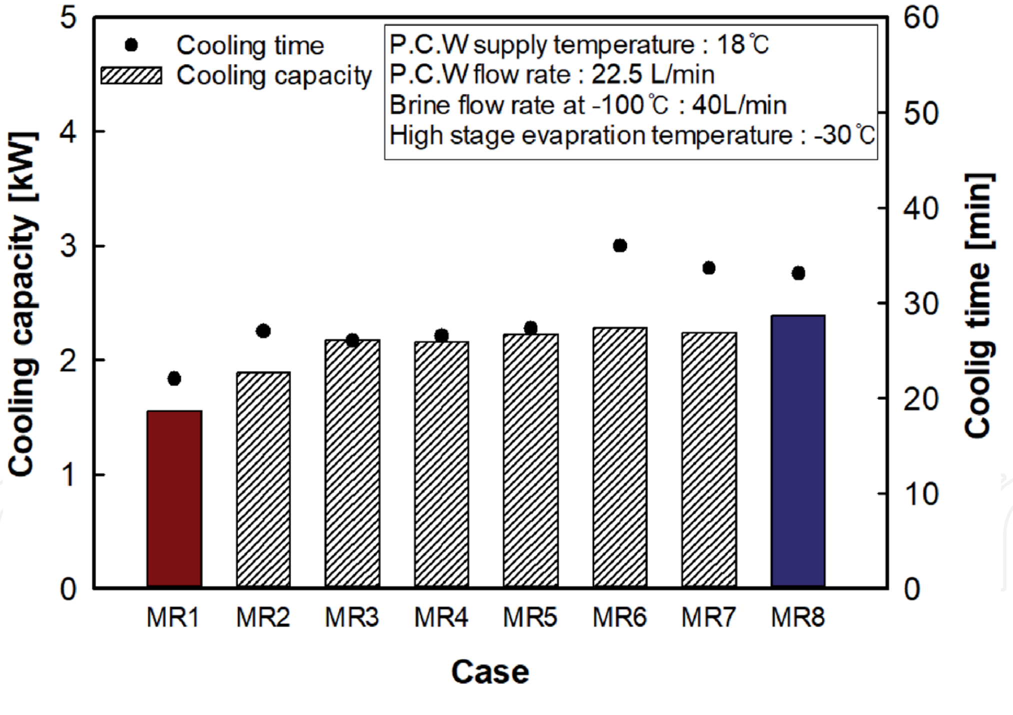

Figure 14.
Cooling capacity and time comparison of various refrigerant composition cases (including R290).

Figure 14 shows a graph by comparing the changes in the cooling capacity and time when the composition of the high boiling refrigerant is changed. As the proportion of the high boiling point refrigerant increases, the cooling capacity shows a decreasing tendency. MR8 shows the highest cooling capacity at the 2.36 kW level, whereas MR1 shows the lowest value with 1.69 kW. However, there is a disadvantage in that the average pressure of the device increases because of the mid/low boiling point refrigerant that has a relatively higher pressure at room temperature as the proportion of the high boiling point refrigerant decreases. Furthermore, the cooling time was defined as the time when the brine supply temperature reaches −100°C, as measured through experiments. As the mass fraction of R290, a high boiling point refrigerant, increased, faster cooling time was achieved.

4.2 Experiments with MR compositions of R600a, R116, R23, and R14

Experiments based on the composition proportion of high boiling point refrigerant were carried out by replacing R290, the high boiling point refrigerant

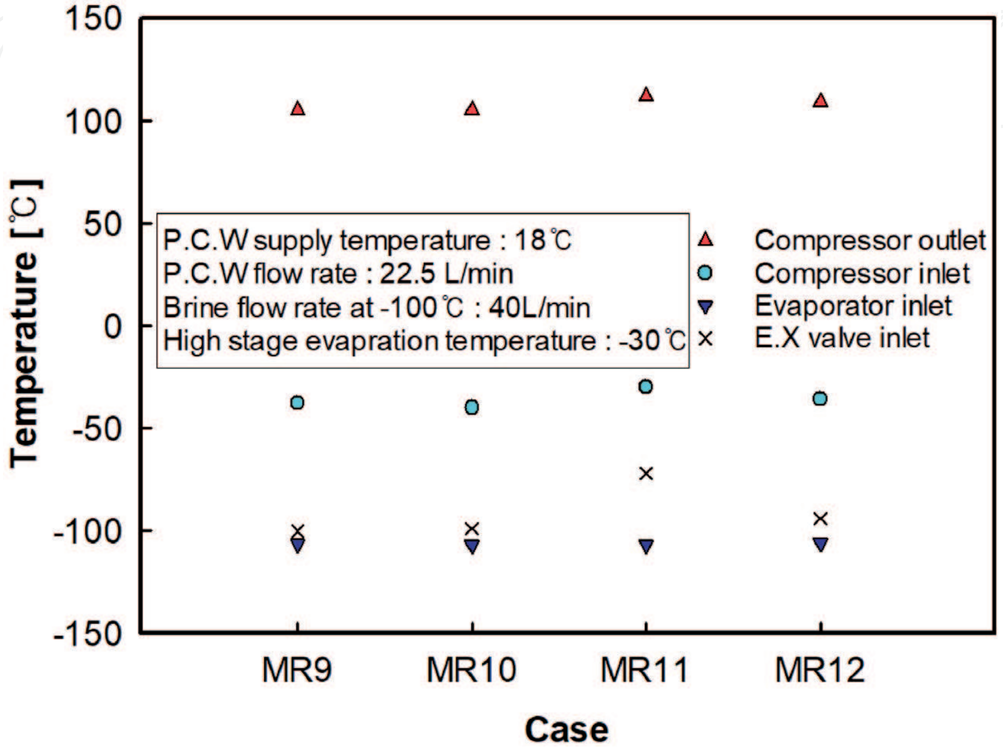

Figure 15.
Temperature comparison of various refrigerant composition cases (including R600a).

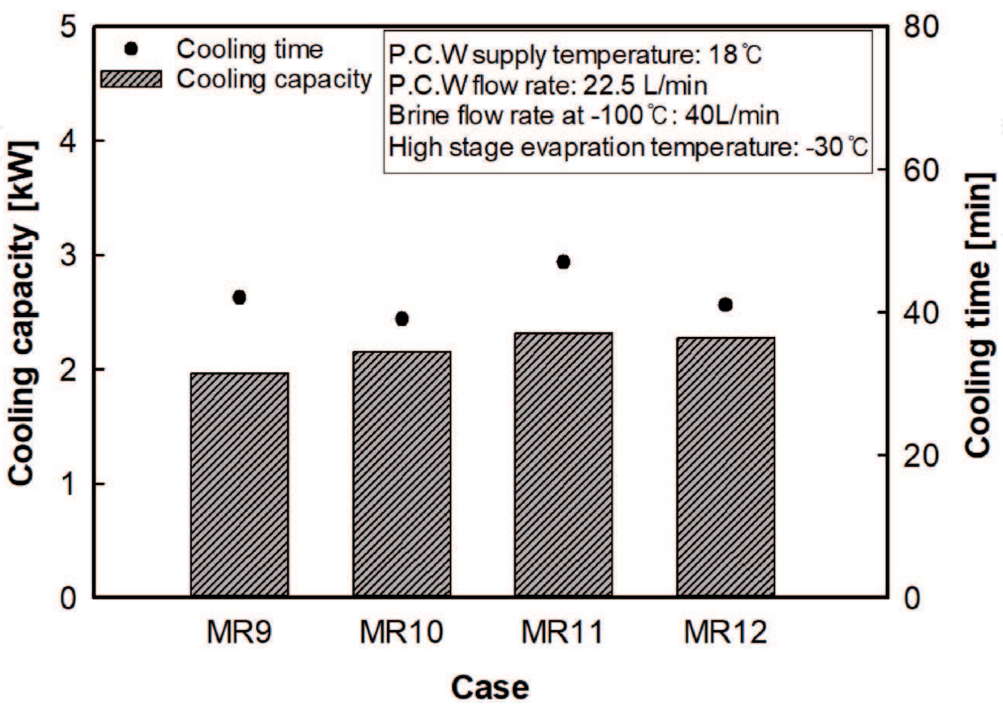

Figure 16.
Cooling capacity and time comparison of various refrigerant composition cases (including R600a).

in the initial refrigerant, with R600a. In this case, the total charging amount in the mass of the refrigerant was the same.

Figure 15 shows the results of experiments performed by adjusting R600a to a mass fraction of 10–35%. Unlike the experimental results of the R290-applied MR, the compressor suction temperature and discharge temperature did not change significantly according to the composition change of the high boiling point refrigerant, in the results of R600a-applied MR experiments. Furthermore, the evaporator inlet temperature was maintained relatively constant between −109.2 and − 108.4°C.

Figure 16 shows the cooling capacity and cooling time according to the decrease of mass ratio of the high boiling point refrigerant. As the mass ratio of the high boiling point refrigerant in the composition of the MR decreased, the cooling capacity increased to 1.94–2.27 kW, and the cooling time was 37–46 min, indicating that the target temperature was reached at a slower rate compared to the MR using R290. It appears that a refrigerant with a boiling point between the high and low boiling points needs to be added to reach the cooling time faster.

5. Conclusions

Four different types of working fluids were selected for low-temperature production of below −100°C, which is required in the semiconductor manufacturing process, and experiments were carried out for R290 and R600a, which are HC refrigerants that show the largest enthalpy differences per unit mass among the high boiling point refrigerants of R290, R600a, R218, and R134a. The effects of changing the composition of the high boiling point refrigerant when the total charging amount is the same in both refrigerant groups was analyzed, and the results show that there is an advantage: as the mass ratio of the high boiling point refrigerant increases, the time for reaching the target temperature decreases, and the average pressure in the device is low. However, as the mass ratio of the high boiling point refrigerant decreases, the cooling capacity increases. The MR shows that the time for reaching the target temperature is short, and the cooling capacity is high when R290 is used as the high boiling point refrigerant among R290 and R600a.

Author details

Jung-In Yoon, Chang-Hyo Son, Sung-Hoon Seol* and Ji-Hoon Yoon
Department of Refrigeration and Air-Conditioning Engineering, College of Engineering, Pukyong National University, South Korea

*Address all correspondence to: seolsh@pknu.ac.kr

References

[1] K. Frost, I. Hua, Quantifying spatiotemporal impacts of the interaction of water scarcity and water use by the global semiconductor manufacturing industry, Water Resour. Ind. 22 (2019) 100115. https://doi.org/10.1016/j.wri.2019.100115.

[2] C.F. Chien, Y.J. Chen, Y.T. Han, Y.C. Wu, Industry 3.5 for optimizing chiller configuration for energy saving and an empirical study for semiconductor manufacturing, Resour. Conserv. Recycl. 168 (2021) 105247. https://doi.org/10.1016/j.resconrec.2020.105247.

[3] M. Newport, Semiconductor Lithography Overview, (n.d.). https://www.newport.com.cn/n/photolithography-overview.

[4] S.K.S. Fan, C.Y. Hsu, C.H. Jen, K.L. Chen, L.T. Juan, Defective wafer detection using a denoising autoencoder for semiconductor manufacturing processes, Adv. Eng. Informatics. 46 (2020) 101166. https://doi.org/10.1016/j.aei.2020.101166.

[5] K.H. Baek, T.F. Edgar, K. Song, G. Choi, H.K. Cho, C. Han, An effective procedure for sensor variable selection and utilization in plasma etching for semiconductor manufacturing, Comput. Chem. Eng. 61 (2014) 20-29. https://doi.org/10.1016/j.compchemeng.2013.09.016.

[6] H. Liang, Y. Chen, X. Xia, C. Zhang, R. Shen, Y. Liu, Y. Luo, G. Du, A preliminary study of SF6 based inductively coupled plasma etching techniques for beta gallium trioxide thin film, Mater. Sci. Semicond. Process. 39 (2015) 582-586. https://doi.org/10.1016/j.mssp.2015.05.065.

[7] H. Abe, M. Yoneda, N. Fujiwara, Developments of plasma etching technology for fabricating semiconductor devices, Jpn. J. Appl. Phys. 47 (2008) 1435-1455. https://doi.org/10.1143/JJAP.47.1435.

[8] L.W. Foo, Radimin, M. Teo, C. Lee, FEA thermal investigation of wafer thinning by plasma etching, 2006 Int. Conf. Electron. Mater. Packag. EMAP. (2006) 815-819. https://doi.org/10.1109/EMAP.2006.4430570.

[9] S.B. Radovanov, P. Corey, G. Angel, D. Brown, Wafer floating potential for a high current serial ion implantation system, Proc. Int. Conf. Ion Implant. Technol. 1 (1999) 482-485. https://doi.org/10.1109/iit.1999.812157.

[10] K. Yasui, M. Osaki, A. Miyamoto, H. Namai, Three-dimensional structure recognition of circuit patterns on semiconductor devices using multiple SEM images detected in different electron scattering angles, Microelectron. Reliab. 108 (2020) 113628. https://doi.org/10.1016/j.microrel.2020.113628.

[11] V. Gadhiraju, Cryogenic Mixed Refrigerant Processes, Springer New York, New York, NY, 2008. https://doi.org/10.1007/978-0-387-78514-1.

[12] O. Podtcherniaev, Performance of throttle-cycle coolers operating with mixed refrigerants designed for industrial applications in a temperature range 110 to 190 K, in: AIP Conf. Proc., AIP, 2002: pp. 863-872. https://doi.org/10.1063/1.1472105.

[13] K.-S. Lee, J.-I. Yoon, C.-H. Son, J.-H. Lee, C.-G. Moon, W.-J. Yoo, B.-C. Lee, Performance Characteristics of a Joule–Thomson Refrigeration System with Mixed Refrigerant Composition, Heat Transf. Eng. (2020) 1-10. https://doi.org/10.1080/01457632.2020.1776995.

[14] ASHRAE, 2009 ASHRAE Handbook-Fundamentals, American Society of Heating, Refrigerating and Air-conditioning Engineer, 2009.

[15] Ji-Hoon Yoon, Performance characteristics of cascade Joule-Thomson Refrigeration cycle with mixed refrigerants composition, Pukyong National University, n.d.